Geofísica Internacional (1997), Vol. 36, Num. 1, pp. 49-54

Hydrogeology and groundwater pollution of Yaqui Valley, Sonora, Mexico

Rodrigo González[1,2], Luis E. Marín[1] and Gustavo Córdova[2]
[1] *Instituto de Geofísica, Universidad Nacional Autónoma de México, Mexico City.*
[2] *Instituto Tecnológico de Sonora, Ciudad Obregón, Sonora, México.*

Received: June 3, 1994; resubmitted: October 16, 1996; accepted: November 18, 1996.

RESUMEN

El uso del sistema G.O.D. fue empleado en la evaluación de la vulnerabilidad del acuífero del Valle del Yaqui, partiendo de datos de pozos perforados y de planos de niveles freáticos. Las descargas de contaminantes fueron identificadas y cuantificadas y el riesgo de contaminación fue calculado analizando la vulnerabilidad del acuífero y las descargas de contaminantes. La zona más vulnerable está en el Oeste y las principales fuentes contaminantes son de origen industrial, agrícola, ganadería y de centros de población. Las áreas de más alto riesgo de contaminación están en la Central, Oeste y Este.

PALABRAS CLAVE: vulnerabilidad de acuíferos, calidad del agua, contaminación de aguas subterráneas, riesgo de contaminación, descargas de contaminantes.

ABSTRACT

We use the G.O.D. criteria to evaluate the vulnerability of the Yaqui Valley aquifer from drill hole data and water table maps. The pollutant loads are identified and quantified and the aquifer pollution risk was calculated from the aquifer vulnerability and the pollution load. The most vulnerable zones are in the West, and the most important contributions of pollutants are from industrial, agricultural, livestock and population centers. The highest aquifer pollution risk areas are Central, West and East.

KEY WORDS: aquifer vulnerability, water quality, groundwater contamination, pollution risk, pollution load.

INTRODUCTION

The Yaqui Valley produces 1'500,000 tons/yr of crops, mainly wheat, corn, soya bean and cotton, plus 35,600 tons/yr of pork, chicken and beef (González and Córdova, 1992). The population is 311,443 habitants (INEGI, 1990). The weather is arid with a rainfall of 300 mm/yr. Up to 1,600 million m^3/yr of runoff is stored in three dams on the Yaqui River. About 340 million m^3/yr of groundwater are produced by 350 wells drilled into the alluvial aquifer. This water is used to 95% in irrigation of 360,000 hectares of land (González, 1993).

The study area is located between 108°53'W to 110° 37'W and 26°53'N to 28°37'N (Figure 1). The aquifer consists of alluvial deposits, in lenses and layers of a mixture of clays and sands to gravels and boulders. The water table level is high in almost all the valley.

AQUIFER VULNERABILITY ASSESSMENT

The aquifer vulnerability was determined using the G.O.D. (Groundwater-Overall lithology-Depth to water table) system for the evaluation of the vulnerability index (Foster and Hirata, 1988). This criterion is based on the evaluation of three input index parameters: groundwater occurrence (confined, unconfined and leaky), overall lithology (consolidation potential and structure as a function of fissuring and permeability) and depth to the water table. Based on the stratigraphic study, five different zones have been identified. These zones were mainly defined by groundwater occurrence and lithology. Thus we have the North subaquifer unit, the South subaquifer unit, and so on (Figure 1). The G.O.D. scale has been used to classify the aquifer subunits. The vulnerability index was computed for all subaquifer units as the arithmetic product (GxOxD) of Groundwater occurrence (G), Overall lithology (O), and Depth to water table (D). See Table 1.

North subaquifer unit

This unit is unconfined covered (Foster and Hirata, 1988). The input index for this type of aquifer is 0.8, using the G.O.D. scale. The upper layers lie on thin highlands, while the lower parts have significant thickness. Underneath the upper layer, a gravel-boulder conglomerate is found with a low clay content (Figure 2). For this lithology type, the input index is 0.5 according to the G.O.D. scale. The water table is found from 5 to 20 m below the surface, and the input index for this depth is 0.8 using the G.O.D. scale. The results are shown in Table 1.

South subaquifer unit

This unit is leaky, and the input index for groundwater occurrence ("G") is 0.6 using the G.O.D. scale. The upper layer is found 20 m below the surface. It consists of a mixture of clay-gravel to a clay-gravel-sand conglomerate. The basement is reached at a depth of 150 m. The unconfined part is close to the sea with deeper layers of sand and little clay (Figure 2). The input index is 0.5 for lithology. The water table is found between 1.5 to 3.0 m; thus the input index for depth is 1.0. The results are shown in Table 1.

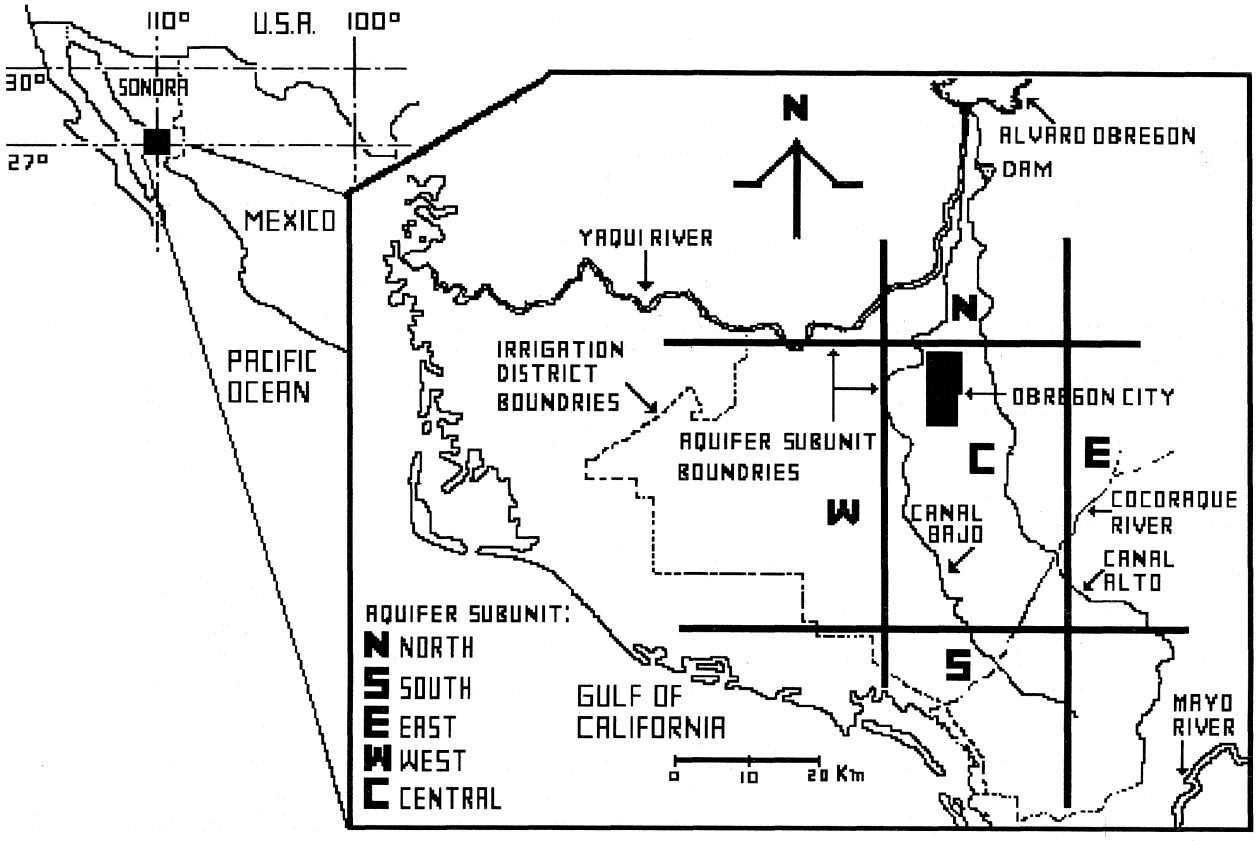

Fig. 1. Study area.

East subaquifer unit

This unit is unconfined, and the input index for this type of aquifer is 1.0. The upper layer consists primarily of a gravel conglomerate associated with clay lenses. The deeper layers contain boulders until the basement. Across the Cocoraque River near the right side of Canal Alto, the lithology consists of clay and sand (Figure 3). For this lithology the input index is 0.6. The water table is found between 10 to 30 m but is 1.5 to 3.0 m near the Cocoraque River; thus the input index for depth is 0.7 (Table 1).

West subaquifer unit

This unit is also unconfined, and the input index for this type of aquifer is 1.0 using the G.O.D. scale. The layer below the surface consists mainly of a sand-gravel conglomerate underlain by clay-gravel in the highlands. A thin clay layer (less than 20 m) is found in the lower part below conglomerate layers of sand with gravel size clasts. This bed has a thickness of 150 m, and is followed by alternating layers of boulders and clay (Figure 3). For lithology the input index is 0.5. The water table is found less than 2.0 m from the surface, and the input index for depth is 1.0 using the G.O.D. scale (Table 1).

Central subaquifer unit

This unit is confined, and the input index for this type of aquifer is 0.4 using the G.O.D. scale. In this area the upper layer consists of 14.0 m of clay with large sand lenses in some areas. The lower layers consist of a conglomerate of clay-sand and clay-gravel to a depth of 150 m. Below this depth boulders are found (Figure 2 and 3). The input index is 0.5 for lithology according to the G.O.D. scale. The water table is found between 1.5 to 3.0 m of the surface; thus the input index for depth is 0.9 (Table 1).

Table 1

Aquifer vulnerability index for the Yaqui Valley aquifer subunits

Parameters	North	South	East	West	Central
Groundwater occurrence	0.8	0.6	1.0	1.0	0.4
Overall lithology	0.5	0.5	0.6	0.5	0.5
Depth to water table	0.8	1.0	0.7	1.0	0.9
Vulnerability index	0.32	0.3	0.42	0.5	0.18
Vulnerability class	Moderate	Moderate-Low	Moderate	Moderate-High	Low

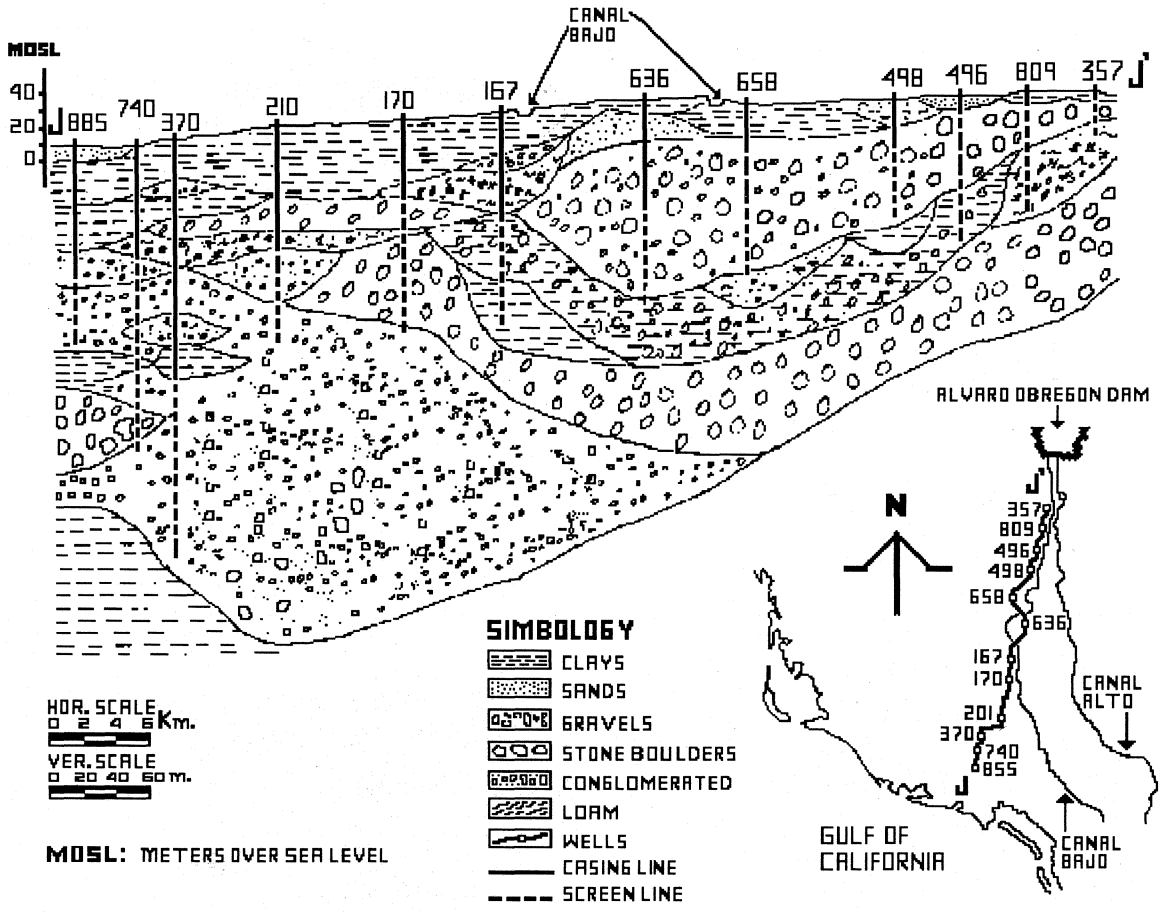

Fig. 2. Geologic section J-J'.

POLLUTION LOAD ASSESSMENT

The economic activities in the study area were compiled from Federal and State Government sources as well as private sources. The components of the subsurface pollution load were estimated from these activities.

Urban and suburban pollution

The liquid and solid pollution load was estimated from Genez and Gervois (1983) at an average of 150 l/person/day of sewage. Genez and Gervois (1983) and Rapoport *et al.* (1983) estimated 0.7 kg/person/day of solid waste. The sewage is collected by a sewer system which discharges into an open ditch also used for collecting the surplus irrigation water. Most small communities do not have sewerage, and the sewage flows into cesspools. Using data by Genez and Gervois (1983), for a population of 311,443 settled in the valley (INEGI, 1990), we compute 46,716 m^3/day of sewage. Sewage often infiltrates the aquifers. Using data by Genez and Gervois (1983), Rapoport *et al.* (1983) and INEGI (1990), the total solid garbage computed is 218 tons/day. The garbage of Obregón City is disposed in a 4.0 m deep landfill. The water table in this area is found at 6.0 m below the surface, which means that the aquifer is highly vulnerable at this point of the valley. The amount and geographic distribution of these pollutant sources (human settlement and garbage disposal) are shown in Table 2, and the pollutant load is shown in Table 3.

Industrial pollution

The data for industrial activities and for the pollution load were compiled. 399 industries are found in this valley; 247 are small, 96 are medium and 56 are large (Cajeme, 1992). The industrial park outside Obregón City contains large industries (Cajeme, 1992), and the smaller industries are located within the city limits. We counted 101 industries that produce garbage and sewage, which probably reaches the aquifer since the sewage flows into the Gulf of California. González and Córdova (1992) report 39,000 m^3/day from industrial sewage and 300 tons/day from collection of domestic and industrial garbage in Obregón City (Cajeme, 1992). The difference between the average human waste and the city record is 82 tons/day, corresponding to industrial and commercial activities. The amounts and geographic distribution of these pollutant sources are shown in Table 2, and the pollutant load is shown in Table 3.

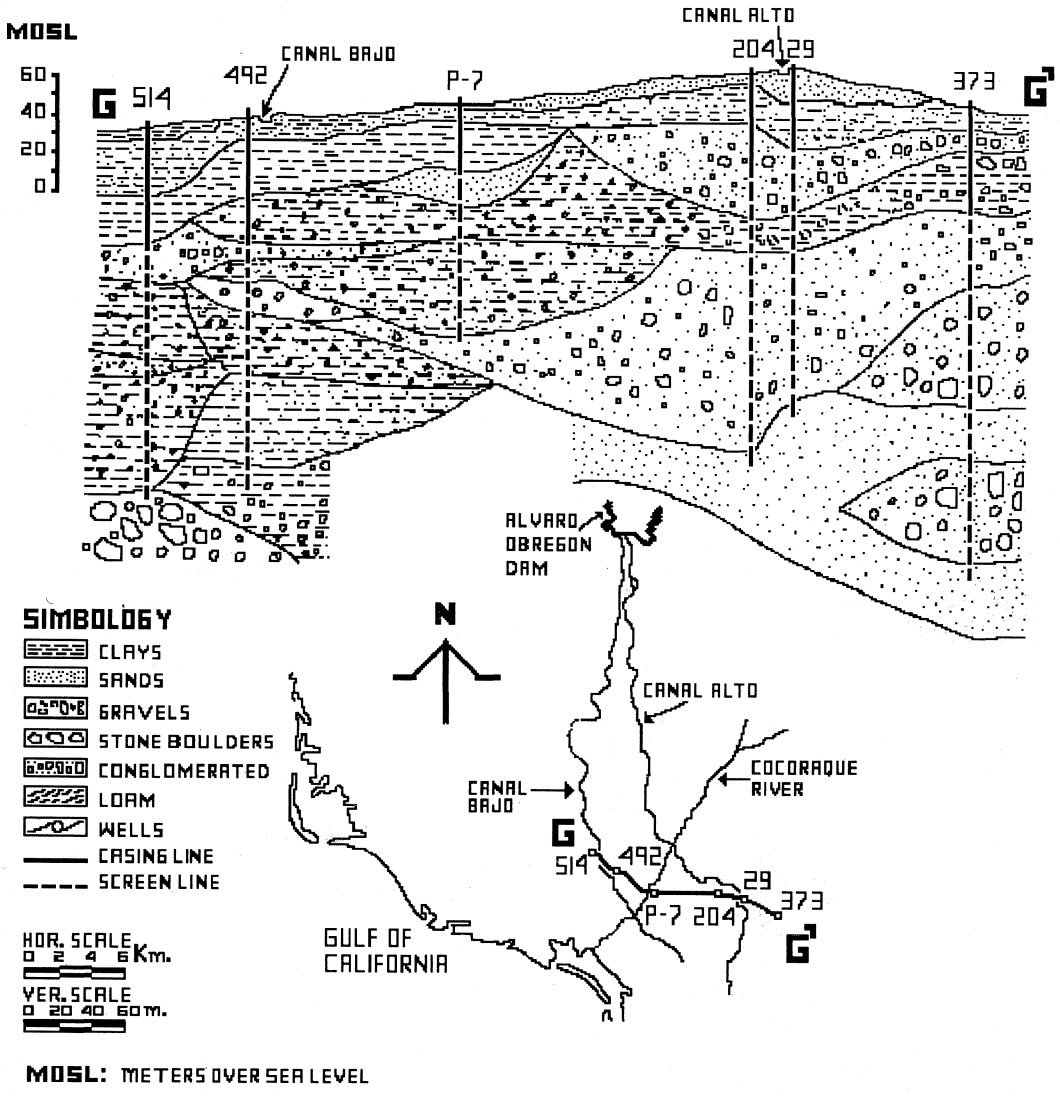

Fig. 3. Geologic section G-G'.

Livestock pollution

Among others, pork and beef are raised in this valley as part of the farming activities. The amount of livestock and farms was compiled by INEGI (1990). The pollution load from this source includes manure and urine, amounting to around 3,200 m³/day from pork, 850 m³/day from beef and 650 m³/day from poultry (González and Córdova, 1992). Thus we compute 4,700 m³/day of pollutant load from this activity. Some of this amount goes into the ground and the rest is drained into the sewer. The amount and geographic distribution of these sources are shown in Table 2, and the pollutant load is shown in Table 3.

Agricultural pollution

The pollution load from fertilizers and pesticides was compiled. According to González and Córdova (1992) about 233 m³/day of fertilizer are used. The most common fertilizers are ammonia, urea and combined N-P-K (Nitrogen, Phosphorus and Potassium). The use of large amounts of pesticides is common in the area. It is estimated that about 0.92 l/hectare of pesticide is applied (González, 1991). For 3 crops/yr at 360,000 hectares/crop, the total amount of pesticide used is in the order of 0.3 m³/day. Pesticides in low concentrations have been found in five wells located in the Central subaquifer, in two wells in the East subaquifer and in one in the North subaquifer in moderate concentrations (González, 1993). García and Meza (1991) found pesticides in food and biologic extracts. The Table 3 show the estimated volume dumped in this valley.

The pollution load index is computed by the product of the potential hazard input index for each pollutant source

(Foster and Hirata, 1988), times the number of sources per subaquifer (Table 2). The output index of pollutant load for each subaquifer is shown in Table 4.

Table 2

Amount of point pollutant sources for Yaqui Valley

Source	North	South	East	West	Central	Total
Human settlement	4	1	5	17	13	40
Garbage disposal	0	0	0	0	1	1
Industry	4	1	3	4	89	101
Livestock	24	2	38	10	35	109
Total	32	4	46	31	138	251

Table 3

Pollutant load emitted by economic activities in Yaqui Valley

Activity	Source	Partial Pollutant (m^3/day)	Pollutant Load Per Activity (m^3/day)
Urban	Sewage	46,716	46,934
	Solid waste	218	
Industry	Sewage	39,000	39,082
	Solid waste	82	
Livestock	Porcine	3,200	4,700
	Bovine	850	
	Aviculture	650	
Agricultural	Fertilizers	233	233
	Pesticides	0.3	
Total			90,949

Table 4

Pollution load index and potential hazard per pollutant source and subaquifer

Source	Potential Hazard Index	North	South	East	West	Central
Industry	0.38	1.52	0. 38	1.1	1.52	33.82
Farming	0.35	8.40	0. 70	13.3	3. 50	12.25
Garbage disposal	0.09	0	0	0	0	0.09
Human settlement	0.23	2.60	0.65	3.2	11.05	8.45
Total		12.52	1.73	17.7	16.07	52.71

AQUIFER POLLUTION RISK

The criteria proposed by Foster and Hirata (1988) were used to estimate the risk of contamination from the interaction between components of aquifer vulnerability and the surface pollution load. We computed the pollution risk of the aquifer as the arithmetic product of the indexes of the aquifer vulnerability times the pollution load. Table 5 summarizes the risk evaluation as follows.

North subaquifer unit

Medium risk as a result of cattle raising activity, and medium vulnerability index for the aquifer.

Southern subaquifer unit

Here the risk is low because of the medium vulnerability index and the low pollutant load.

Eastern subaquifer unit

High risk index as a result of livestock activity and high pollutant load near the Irrigation District, just across Cocoraque River, even though this subaquifer unit has a moderate vulnerabilty index.

Western subaquifer unit

Rates a high risk of contamination due to the pollutant load and the high vulnerability index.

Central subaquifer unit

Has a low vulnerability index but a high pollutant load. This is because most activities are concentrated in this area.

Table 5

Pollutant hazard index for each of the subaquifer units

Subaquifer	North	South	East	West	Central
Vulnerability Index	0.32	0.30	0.42	0.50	0.18
Pollutant Load Index	12.52	1.73	17.69	16.07	52.71
Pollutant Risk Index	4.01	0.52	7.43	8.03	9.49
Potential Danger Class	Medium	Low	High	High	High

CONCLUSIONS

The Yaqui Valley aquifer is more vulnerable in the West and less in the Central subaquifer units. The main pollutant sources for this aquifer are livestock, industry and agriculture. We find that the pollution risk is high in the Central, West and East, and low in the South subaquifer units. This is a consequence of the concentration of economic activities as well as of the population. A medium

pollution risk is proposed for the North subaquifer unit. These results suggest that priorities in terms of research and regulation should be given to the Central, West and East subaquifer units.

ACKNOWLEDGMENTS

This report was supported by grants from Instituto Tecnológico de Sonora, Instituto Mexicano de Tecnología del Agua and Comisión Nacional del Agua (ITSON-IMTA-CNA Project Anexo 13), and by Consejo Nacional de Ciencia y Tecnología (Project 1630P-T and Doctoral Grant 96137).

BIBLIOGRAPHY

CAJEME, 1992. Anuario estadístico del Municipio de Cajeme. Dirección municipal de planeación del desarrollo y gasto público. H. Ayuntamiento del Municipio de Cajeme. Cd. Obregón, Sonora, México. 75 pp.

FOSTER, S. and R. HIRATA, 1988. Groundwater pollution risk assessment. World Health Organization. Pan American Health Organization. Pan American Center for Sanitary Engineering and Environmental Sciences (CEPIS). Lima , Perú. 79 pp.

GARCIA, B. L. and M. M. MEZA, 1991. Principales vías de contaminación por plaguicidas en neonatos-lactantes residentes en Pueblo Yaqui, Sonora. Instituto Tecnológico de Sonora. Journal ITSON-DIEP, v 1,2. p. 33-42

GENEZ, R. C. and Y. H. GERVOIS, 1983. Medicina preventiva, salud pública e higiene. Editorial LIMUSA, México. p. 42-43

GONZALEZ, R., 1993. Evolución de la salinidad y contaminación por agroquímicos en el acuífero del Valle del Yaqui, Sonora, México. Report of project by Instituto Tecnológico de Sonora for Instituto Mexicano de Tecnología del Agua and Comisión Nacional del Agua. Cd. Obregón, Sonora, México. 68 pp.

GONZALEZ, R., 1991. Contaminación por plaguicidas en el acuífero del Valle del Yaqui, Sonora. Master's Thesis. Instituto Tecnológico de Sonora. Ciudad Obregón, Son., Méx. 90 pp.

GONZALEZ, R. and G. CORDOVA, 1992. Evaluación del riesgo de contaminación de las aguas subterráneas del Valle del Yaqui, Sonora, México. Project report of Instituto Tecnológico de Sonora. Cd. Obregón, Sonora, México. 70 pp.

INEGI, 1990. Sonora. Resultados definitivos tabulados básicos Tomo 1. XI censo de población. Instituto Nacional de Estadística, Geografía e Informática. México, D.F., México.

RAPOPORT, H. E, B. E. DIAZ and M. S. LOPEZ, 1983. Aspectos de la ecología urbana en el Estado de México. Editorial. LIMUSA. México D.F., México. p. 6-9

Rodrigo González[1,2], Luis E. Marín[1] and Gustavo Córdova[2]

[1] Instituto de Geofísica, UNAM. Circuito Exterior, Cd. Universitaria, Coyoacán, 04510 México, D.F., México

[2] Instituto Tecnológico de Sonora. 5 de Febrero 818 Sur, 85000 Cd. Obregón, Sonora, México

Geofísica Internacional (1997), Vol. 36, Num. 1, pp. 55-60

The detection of electromagnetic processes in the ionosphere caused by seismic activity

S.V.Koshevaya[1], R. Pérez-Enríquez[2] and N. Ya. Kotsarenko[2]
[1] *Instituto Nacional de Astrofísica, Optica y Electrónica (INAOE), Puebla, Mexico.*
[2] *Depto. de Física Espacial, Instituto de Geofísica, UNAM, México, D. F., Mexico.*

Received: February 22, 1996; accepted: June 19, 1996.

RESUMEN

El propósito del presente artículo es el de presentar una nueva dirección en la investigación de terremotos por medio de procesos electromagnéticos en la ionosfera causados por actividad sísmica. Con este fin, se consideran las principales perturbaciones de la ionosfera causadas por terremotos, se analizan los mecanismos de conexión entre la litosfera y la ionosfera, y se discute la posibilidad de establecer una alarma para la ocurrencia de terremotos por medio de métodos espaciales y terrestres.

PALABRAS CLAVE: Ionosfera, actividad sísmica.

ABSTRACT

The purpose of this article is to present a new direction in the investigation of earthquakes through the research of electromagnetic processes in the ionosphere caused by seismic activity. To accomplish this objective, the main perturbations of the ionosphere caused by earthquakes are considered, the connection mechanisms between the lithosphere and the ionosphere are analysed, and the possibility to establish a warning for the occurrence of earthquakes by means of space and ground methods is discussed.

KEY WORDS: Ionosphere, seismic activity.

1. INTRODUCTION

The prediction of earthquakes and volcanic eruptions remains largely an unsolved problem. Disastrous earthquakes, which occur from 100 to 200 times per year, are a hazard for every other inhabitant of our planet. Annually, thousands of people lose their lives under collapsed buildings, in fire and tsunamis caused by earthquakes.

2. PERTURBATION OF THE IONOSPHERE CAUSED BY EARTHQUAKES

A system of monitoring the occurrences of earthquakes from space must rely on the connection between the lithosphere, the ionosphere and the magnetosphere of the Earth. This connection may be established either from ground or from space.

There is at present factual material that shows evidence of a response in the ionosphere from seismic activity. Above the epicentre of a future earthquake, at altitudes from about 400 km to about 1000 km in the ionosphere, there appear macroscopic changes of the ionospheric parameters prior to the occurrence of the earthquake.

The presence in the ionosphere of precursors of earthquakes affords the possibility in principle of prediction by remote space-ground methods. The study of the influence of the seismic activity on the ionosphere began more than 30 years ago (see references). Some of the observations are the following.

- An anomaly in the absorption of cosmic ray emission after the 1960 earthquake in Chile lasted for 6 days (Warwick, 1963).
- Strong changes in the parameters of the ionosphere caused by the large earthquake in Alaska in 1964 (Davies and Barker, 1965).
- The discovery by Tarantsev and Birfeld (1973) that acoustic waves are involved in the connection between seismic activity and the ionosphere.

Since 1975, when the Soviet-French experiment "Arkad" was active in the ionosphere and the magnetosphere, processes caused by seismic activity were observed. The identification of these processes took place not at the time of the earthquake but hours or days before. Similar phenomena were observed on "Intercosmos 19", "Intercosmos 24", "OGO-6", "Nimbus", "GEOS 1", "GEOS 2", and other satellites. We propose five main types of ionospheric perturbations that accompany earthquakes.

(1). Variations of electric and magnetic fields.

The variations of electric δE and geomagnetic δH fields, as well as their frequency ranges are:

$$\delta E \approx 10^{-7} - 10^{-2} V/m, f \approx 10^{-2} - 10 Hz,$$
$$\delta H \approx 10^{-4} - 10^{-1} nT, f \approx 10^{-2} - 10 Hz .$$

Variations of the electric field caused by earthquakes were first proposed by Chernyavskiy (1925). Variations of the magnetic field δH were observed in Kazan in 1880.

(2). Perturbations of the electromagnetic waves at extremely low (ELF) and very low frequencies (VLF) as follows.

(ELF) $f \approx 10^{-2} - 10^{2}\,Hz$, I_f maximum at $f \approx 8Hz$;

(VLF) $f \approx 10^{2} - 10^{5}\,Hz$, I_f maximum at $10\text{-}15KHz$;

where I_f is the intensity of the electromagnetic perturbation.

(3). Perturbations of density and temperature of the ionosphere plasma in the F- and E -layers. In some cases the density may increase and in others it may decrease.

The observed values of the concentration in F-layer are:

$$\delta n / n \approx 10^{-3} - 10^{-1},$$
$$\delta T > 0, \delta T / T \approx 10^{-2} - 10^{-1}$$

where δn is the density change and T is the temperature.

(4). Increases of the intensity of luminescence of the ionosphere at the main spectral wavelengths of atomic oxygen λ = 5577 Å, 6300 Å.

Ionospheric luminescence before earthquakes is well known. It occurred above Rome in 373 BC. This phenomenon has also been reported above Tashkent and Spitak, Armenia during the 1966 and 1988 earthquakes, respectively.

(5). Flows of geoactive particles in the magnetosphere.

It turns out that the variations of the E, H fields, the low-frequency oscillations and the presence of flows of geoactive particles appear as a rule some hours before and up to the beginning of the earthquake, whereas the variations of the density, the temperature and the optical emission may appear one or two days before and until the occurrence of the earthquake.

Other phenomena have been observed, such as anomalies in the propagation of radio waves above the epicentre of earthquakes (Fuks and Shubova, 1994); perturbation of the sporadic Es-layer emission in the ionosphere; geochemical and biological processes in the seas, oceans, and others.

3. MAIN MECHANISMS OF CONNECTION BETWEEN LITHOSPHERE AND IONOSPHERE

At present no consistent theory has been developed about the connection between the lithosphere and the ionosphere. The mechanisms of interaction between these regions are not fully understood. However, it is clear that the main mechanisms of transfer of energy from the lithosphere to the ionosphere must be acoustic or electromagnetic.

The mechanics of the lithosphere-ionosphere connection involve the transformation of acoustic waves into magnetoacoustic and Alfvén waves (Figure 1). The oscillations of the Earth's surface excite acoustic and gravity waves in the atmosphere. After they spread upwards they are transformed into Alfvén and magnetoacoustic waves. They appear as electromagnetic oscillations of low frequency. Consider the equations of the theory of elasticity for the lithosphere:

$$\rho \frac{\partial^2 \vec{U}}{\partial t^2} = \lambda \nabla\, div\, \vec{U} + \mu \Delta \vec{U} + \vec{F} \qquad (1)$$

where $\vec{U}$ is the acoustic displacement, ρ is the density, λ and μ are the coefficients of elasticity, and $\vec{F}$ is the force of electroacoustic origin which is the source of excitation of acoustic waves. The equations of hydrodynamics for the atmosphere are:

$$\rho\left(\frac{\partial \vec{v}}{\partial t} + (\vec{v}\cdot\nabla)\vec{v}\right) = -\nabla P + \rho \vec{g}, \qquad (3)$$

$$\frac{\partial \rho}{\partial t} + div\ (\rho \vec{v}) = o, \qquad (4)$$

$$P = P(\rho, T)\ , \qquad (5)$$

where $\vec{v}$ is the velocity, P is the pressure, $\vec{g}$ is the acceleration of gravity and T is the temperature, and the equations of magnetohydrodynamics for the ionosphere are:

$$\rho\left(\frac{\partial \vec{v}}{\partial t} + (\vec{v}\cdot\nabla)\vec{v}\right) = -\nabla\left(p + \frac{H^2}{8\pi}\right) + \frac{(\vec{H}\cdot\nabla)\vec{H}}{4\pi}\rho\vec{g}, \qquad (6)$$

$$rot\vec{H} = \frac{4\pi}{c}\vec{j}, \vec{j} = \hat{\sigma}\cdot\vec{E}, \qquad (5)$$

$$rot\vec{E} = -\frac{1}{c}\frac{\partial \vec{H}}{\partial t}, \qquad (7)$$

where $\vec{E}$, $\vec{H}$ are electromagnetic fields, and $\hat{\sigma}$ is the conductivity tensor of the ionosphere. It is necessary to introduce boundary conditions, which requires computer modelling.

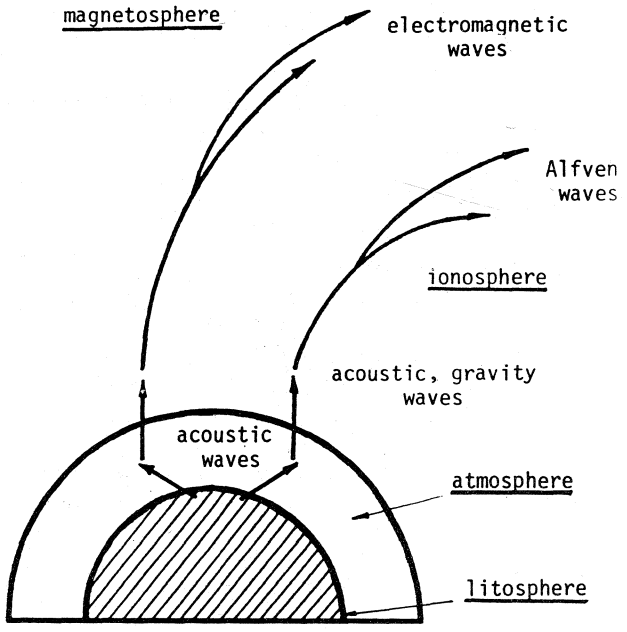

Fig. 1. Connection between the lithosphere and the ionosphere involving the transformation of acoustic waves into Alfvén waves, magnetoacoustic waves and others.

Another model was proposed by Schuman 1952, (Figure 2). The nonstationary electrical currents in the lithosphere are connected with the horizontal motion of the ground having a relatively high conductivity. According to Maxwell's equations, it becomes almost instantly apparent in the ionosphere. Suppose that there is a known current determined by geophysicists in a region of the lithosphere. Then there should exist corresponding electromagnetic fields in the ionosphere (Molchanov *et al.*, 1993). If the Earth's surface and the ionosphere constitute an electromagnetic resonator (Schuman's resonator), this current excites electromagnetic oscillations. Thus the maximum of low frequency electromagnetic oscillations found through satellite observations occurs approximately at a frequency f≈8Hz, which corresponds to the first characteristic frequency of Schuman's resonator (Schuman, 1952):

$$f \approx \frac{c}{2\pi R}\sqrt{n(n+1)}, \qquad n = 1,2,3 \tag{8}$$

where R is the radius of the Earth (Figure 2).

The maximum of VLF oscillations falls in the frequency range of $f \approx$ 10 -15 KHz, corresponding to transverse oscillations of the resonator formed by the surface of the Earth and the ionosphere:

$$f \approx \frac{nc}{L}, \quad n = 1,2,3 \tag{9}$$

where L is the altitude of the D - layer of the ionosphere. The spectrum of the oscillations is shown in Figure 2. The observations give the same frequencies (Figure 3).

The use of a space system for monitoring seismic activity presents some difficulties. It is necessary to take into account:

(a) changes in solar activity capable of generating similar signals in the ionosphere. These are considered by using available solar geophysical data;

(b) anthropogenic factors (artificial explosions, launching of rockets and so on);

(c) the short time available for the treatment of satellite information.

Plasma experiments may be carried out in the ionosphere, above the area of seismic activity, during periods of months or years, but the effects of seismic activity on ionospheric parameters will be felt minutes or hours, at best, before the earthquake.

4. WARNING FOR EARTHQUAKES

None of the satellites was designed for the investigation of processes in the ionosphere caused by seismic activity. The results that have been obtained in this field are fortuitous. The Ukrainian space project "Warning" whose scientific leader until 1995 was one of us (N. Y. K.) will be devoted to these investigations, and specifically the electromagnetic processes in the ionosphere caused by seismic activity (Kotsarenko *et al.*, 1995). This project is in charge of the Kiev National University (Department of Astronomy and Space Physics) and Pivdenne (Yuzhnoe) Design Bureau (Dnepropetrowsk). The participating countries are Russia, Austria, Hungary, Poland, Czech Republic, Romania, France, Germany, and Ukraine. The project includes rocket assembly, rocket and launching facilities; ground-based flight control with telemetry and communication links and stations; ground-based high-performance working in close connection with the spaceborne computer during data acquisition and processing; and a network of seismological stations and other ground instrumentation such a ionospheric and magnetic stations, optical facilities for the ground-based measurements and so on.

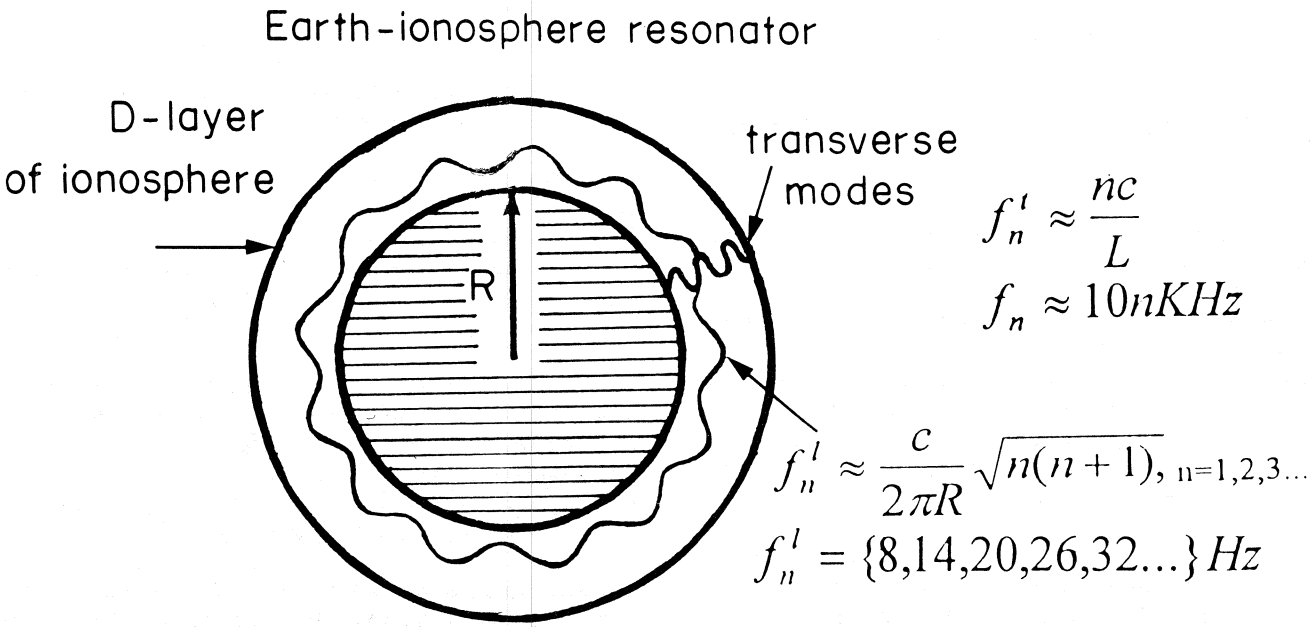

Fig. 2. Schuman resonator of the Earth-ionosphere cavity.

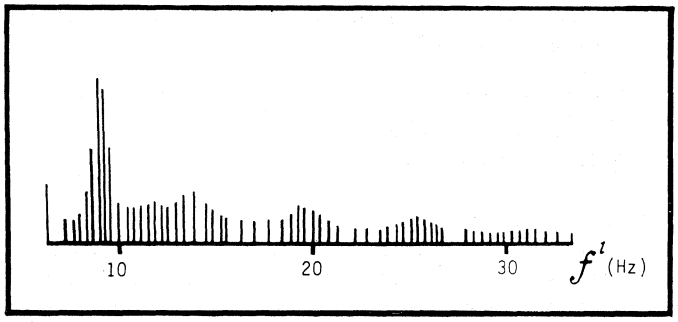

Fig. 3. The spectrum of Schuman oscillations obtained from ground observations.

The parameters of the space platform are shown below.

orbit	- circular, 600 km
declination	- 74 degrees
composition	- a satellite +2 sub-satellites
weight	- satellite-1500 kg; sub-satellite-100 kg
Satellite orientation accuracy	- better than 15 Deg
angular stabilisation velocity	- less than 0,05 Deg/s
period of active operation	- more than 1 year
rocket type	- Cyclone
tentative launching time	- 1998

The scientific payload of the spacecraft will contain the following equipment:

- Wave complex for measuring electric and magnetic fields;
- Instrumentation for measuring temperatures and concentrations of ionospheric plasma;
- Ionosonde radio-spectrometer for measuring electron concentration profiles below the F- layer maximum;
- System for measuring optical emissions of the ionosphere;
- Spectrometers of energetic particles (electrons, protons, ions);
- Two-frequency transmitter (150/400 MHz) for tomographic sounding of the ionosphere. The scheme of the space control system is shown in Figure 4.

The global character of the seismic problem calls for remote sensing methods of investigation. Only remote methods (mainly space borne) can ensure obtaining the necessary information from large regions with sufficient time resolution (Mc Farland *et al.*, 1990; Alishouse *et al.*, 1980; 1990; Barrett *et al.*, 1981; Gasiewski *et al.*, 1990; Neale *et al.*, 1990; Petty and Kotsaros, 1990; Westwalter *et al.*, 1989).

It is important to use appropiate ground control such as the mountain landmarks or the ocean coast. Radiometers, bolometers, and magnetometers on mountain tops will provide a reliable surveillance of the environment. Sensing from space does not always provide the temporal and spatial resolution required. Furthermore, it is rather expensive and requires equipment calibration, which is impossible without the use of ground control. The radiometers, bolometers, and magnetomer remote-sensing systems have certain advantages when compared with other spaceborne methods:

(1). The space remote sensing does not always provide good space-time resolution (Basharrimov *et al.*, 1970; Hollinder *et al.*, 1990).

(2). The space remote sensing needs calibration by ground observations (Hollinder *et al.*, 1990).

(3). The spaceborne sensing does not always provide fast control since it depends on weather conditions (Goodbelret, 1990).

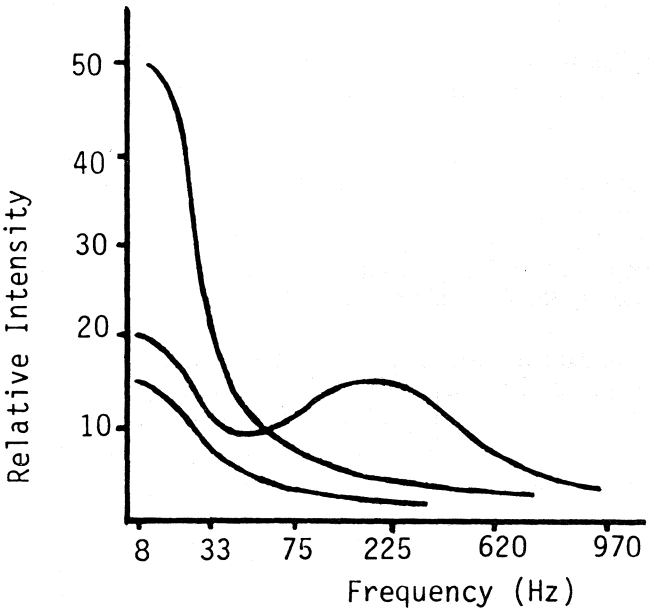

Fig. 4. The spectrum of Schuman oscillations obtained from satellite observations.

A Mexican project by Instituto Nacional de Astrofísica, Optica y Electrónica-INAOE, together with Instituto de Geofísica-UNAM devoted to creation to a radiometer, bolometer, and magnetomer remote-sensing system and computer warning for earthquakes is being proposed as follows.

The radioelectronic system will be created on the basis of integrated low-noise receivers (Koshevaya *et al.*, 1982) with antennas in different frequencies controlled by a personal computer. The data acquisition, the observation analysis, and the forecast of weather phenomena are based on the computer and spatial programs. The system will be based on an analogue system created at the Saturn Institute in Kiev (Chmil *et al.*, 1995). This Institute has participated in design of new receivers for radiotelescopes and remote space communication,some of which are working

successfully on the Ratan radiotelescope and in the centre of remote space communication in Jevpatoria, Ukraine (Bakitko *et al.*, 1993).

This ground-based remote-sensing system has a number of advantages when compared with satellite sensing:

(1) The use of identical elements gives the possibility to eliminate device errors, to increase reliability and precision of measurements and to simplify calibration.

(2) The system is not as expensive as space systems, as it uses identical integrated elements with a small energy consumption.

(3) The use of mountain landmarks with simultaneous meteorological stations and a net of radiometers, bollometers, and magnetometers enables us to increase the number of observations and to improve control of parameters of sensing.

(4) The proposed system is ecologically safe, indestructible and non-polluting (Guiraud, 1979; Snider *et al.*, 1980).

The remote-sensing system is based on measuring the characteristics of radioheating radiation of the atmosphere and ocean in the microwave range and low frequency magnetic fields. The basic parameters are the radiobrightness temperature in the microwave range, the temperature contrasts and the value of magnetic field.

In the remote-sensing system, the use of new types of integrated elements (Chmil *et al.*, 1995; Bakitko *et al.*, 1993) is considered, with low-cost technology and a new method for measuring ocean parameters and vertical profiles of wind velocity.

4. CONCLUSION

Measuring the radiobrightness temperature and magnetic fields may provide warning capabilities for earthquakes. Microwave radiation at all frequencies generated under the epicentre causes the radiobrightness temperatures of the ionosphere and atmosphere as well as the surface at the epicentre to change very rapidly. This provides the possibility together with seismic and meteorological stations, to monitor a region for future volcanic and seismic phenomena.

We conclude that, in principle, the accumulated experience through observations on the ground and in space may raise the possibility of creating a global space-ground system for detection and prediction of earthquakes.

BIBLIOGRAPHY

ALISHOUSE, J. C., J. B SNIDER, E. D. R. WESTWATER, C. T. SWIFT, C.S. RUF, S.A. SNYDER, J. VONGSATHORN and R.R. FERRARO, 1980. Determination of Ocean Total Precipitation Water from the SSM/I. *IEEE Trans. on Geoscience and Remote Sensing, 28*, 817-822.

ALISHOUSE, J.C., R. FERRARO and J.V. FIORE, 1990. Influence of Oceanic Rainfall Properties from the Nimbus-7 SMMR. *J. Appl. Meteor., 29*, 551-559.

BAKITKO, R.V.M., M.B. VASILYEV, A.S. WINITZKI, *et al.*, 1993. Radiosystems of Remote Space Communication. Moscow. Radio and Communication Publishing House, 1993, 328p. (in Russian).

BARRETT, E. C. and D. W. MARTIN, 1981, The Use of Satellite Data in Rainfall Monitoring. Academic Press. 340p.

BASHARRIMOV, A. E., A. S. GURVICH, L. T. TUCHKOV and K. S. SHIFRIN, 1970. The Terrestrial Thermal Radio-Emission Field. *Atmos. Ocean. Phys., 6*, 210-218.

CHERNYAVSKY, E., 1925. Electric Storms. Proc. of CASU, p.157. (in Russian).

CHMIL, V. M., K. S. SUNDUCHKOV and L. S. NASARENKO, 1995. The Border Multichannel Radiometrical Complex for the Distant Sounding of the Earth from the Space RMC/KII. Proc. of the 5th International Symposium on Recent Advances in Microwave Technology (ISRAMT'95), Kiev, p.141-146.

DAVIS, K. and D. BARKER, 1965. Ionospheric Effects Observed Around the Time of the Alaska Earthquake of March, 1964. *J. Geophys. Res., 70*, 2551-2553.

FUKS, I. M. and R. S. SHUBOVA, 1994. ELF-signal anomalies as a response of the lower ionosphere to conductivity change in the atmosphere. *Geomagnetism and Aeronomy, N2*, 130.

GASIEWSKI, A. J., J. W. BARRETT, P. G. BONANNI and D. H. STAELIN, 1990. Aircraft-Based Radiometric Imaging of Tropospheric Temperature and Precipitation Using the 118.75 GHz Oxygen Resonance. *J. Appl. Meteor., 29*, 620-632.

GOODBELRET, M. A., 1990. Ocean Surface Wind Speed Measurements of the Special Sensor Microwave/Imager (SSM/I). *IEEE Trans. Geoscience, Rem. Sens., 28*, 823-828.

GUIRAUD, F. O., 1979. A Dual-Channel Microwave Radiometer for Measurement of Precipitable Water Vapor and Liquid, *IEEE Trans. Geoscience Electr.,.GE-17*, 551-554.

HOGG, D. C., 1980. Design of a Ground-Based Remote Sensing System Using Radio Wavelengths to Profile Lower Atmospheric Winds, Temperature and Humidity. *Remote Sensing of Atmosphere and Oceans*, Academic Press Inc., 313-364.

HOLLINDER, J. P., J. L. PEIRCE and G. A. POE, 1990. SSM/I Instrument Evaluation. *IEEE Trans. Geoscience Rem. Sens. 28,* 781-789.

KOSHEVAYA, S. V., B. N. EMELYANENKOV and L. G. GASSANOV, 1982. Integrated Circuits for the MM Range. *Radioelectr. Com. Systems, 25,* 14-31.

KOTSARENKO, N. Ya., V. E. KOREPANOV and V. N. IVCHENKO, 1995. The Investigation of the Ionosphere Precursors of Earthquakes (Experiment "Warning"). *Kosmichnaya nauka i technologiya, 1,* 93-96. (in Russian).

MOLCHANOV, O. A., O. A. MAZHAEVA, A. N. GOLIAVIN and M. HAYAKAWA, 1993. Observation by the Intercosmos-24 Satellite of ELF-VLF Electromagnetic Emission Associated with Earthquakes. *Ann. Geophysics 11,* 431-440.

McFARLAND, M. J., R. L. MILLER and C. M. U. NEALE, 1990. Land-Surface Temperature Derived from the SSM/I Passive Microwave Brightness Temperatures. *IEEE Trans. Geoscience Rem. Sens., 28,* 939-945.

NEALE, C.M.U., M.J. McFARLAND and KAI CHANG, 1990. Land-Surface-Type Classification Using Microwave Brightness Temperatures from the Special Sensor Microwave/Imager. *IEEE Trans. Geoscience Rem. Sens., 28,* 829-838.

PETTY, G.W. and K.B. KATSAROS, 1990. Precipitation Observed over the South China Sea by the Nimbus-77 Scanning Multichannel Microwave Radiometer during Winter MONEX. *J. Appl. Meteor. 29,* 273-287.

SCHUMAN, W.O., 1952. Über die strahlungslosen Eigenschwingungen einer leitenden Kugel, die von einer Luftschicht und einer Ionosphärenhülle umgeben ist. *Z. Naturforsch. 7a,* 149-154.

SNIDER, J.B., F.O. GUIRAND and D.C. HOGG, 1980. Comparison of Cloud Liquid Content Measured by Two Independent Ground Based Systems. *J. Appl. Meteor., 19,* 577-579.

TARANTSEV, A. and Ya BIRFILD, 1973. Discovery: Influence of the Seismic Activity on Ionosphere by Acoustic Waves. *Short description of discoveries, 128,* 157. (in Russian).

WARWICK, J. W., 1963. Radioastronomical Techniques for the Studies of the Atmosphere. (Ed. by J. Aarons). North Holland, Amsterdam p. 400.

WESTWALTER, E. D., 1989. Combined Ground-and Satellite Based Radiometric Remote Sensing. *In:* "RSRM" 87: Advances in Remote Sensing Retrieval Methods, DEEPAK Publishing, 215-228.

S.V. Koshevaya[1], R. Pérez-Enríquez[2] and N. Ya. Kotsarenko[2]

[1] *Instituto Nacional de Astrofísica, Optica y Electrónica (INAOE), P.O.BOX 518&216, 7200 Puebla, México.*
e-mail: svetlana@inaoep.mx

[2] *Depto. de Física Espacial, Instituto de Geofísica, UNAM, Coyoacán, 04510 México, D. F., México.*